Award Number: W81XWH-13-1-0160

TITLE: FRET Imaging Trackable Long-Circulating Biodegradable Nanomedicines for Ovarian Cancer Therapy

PRINCIPAL INVESTIGATOR: Jindřich Kopeček

CONTRACTING ORGANIZATION: The University of Utah
Salt Lake City, UT 84112-9023

REPORT DATE: September 2014

TYPE OF REPORT: Annual

PREPARED FOR: U.S. Army Medical Research and Materiel Command
Fort Detrick, Maryland 21702-5012

REPORT DOCUMENTATION PAGE

Form Approved
OMB No. 0704-0188

1. REPORT DATE	**2. REPORT TYPE**	**3. DATES COVERED**
Sept 2014	Annual	01 Sept 2013 – 31 Aug 2014

4. TITLE AND SUBTITLE
FRET Imaging Trackable Long-Circulating Biodegradable Nanomedicines for Ovarian Cancer Therapy

5a. CONTRACT NUMBER

5b. GRANT NUMBER
W81XWH-13-1-0160

5c. PROGRAM ELEMENT NUMBER

6. AUTHOR(S)
Jindřich Kopeček

E-Mail: Jindirch.Kopecek@utah.edu

5d. PROJECT NUMBER

5e. TASK NUMBER

5f. WORK UNIT NUMBER

7. PERFORMING ORGANIZATION NAME(S) AND ADDRESS(ES)
The University of Utah

Salt Lake City, UT 84112-9023

8. PERFORMING ORGANIZATION REPORT NUMBER

9. SPONSORING / MONITORING AGENCY NAME(S) AND ADDRESS(ES)
U.S. Army Medical Research and Materiel Command
Fort Detrick, Maryland 21702-5012

10. SPONSOR/MONITOR'S ACRONYM(S)

11. SPONSOR/MONITOR'S REPORT NUMBER(S)

12. DISTRIBUTION / AVAILABILITY STATEMENT
Approved for Public Release; Distribution Unlimited

13. SUPPLEMENTARY NOTES

14. ABSTRACT Enter a brief (approximately 200 words) unclassified summary of the most significant finding during the research period

The major goal of the proposed project is to develop a novel FRET imaging strategy, which permits visualizing the biodegradation of copolymer-drug conjugates at the body, tissue and cell levels in real time. The information will initiate the understanding of *in vivo* behavior of biodegradable polymers and support the design of highly efficient drug delivery systems. In the first year of the project we have synthesized numerous FRET trackable biodegradable *N*-(2-hydroxypropyl)methacrylamide (HPMA) copolymer conjugates that were labeled with Cy3 and/or Cy5, conjugates that contained epirubicin and performed click reactions for chain extension to manipulate their molecular weight. The conjugates were characterized by physicochemical methods and in vitro using human ovarian carcinoma cells. FRET technique was used to investigate the conjugates at cellular level. We achieved correlation of the FRET signal on one hand with the level of cathepsin B expression and with the intracellular degradation of the conjugates on the other hand. In fluorescence spectrophotometry experiments we have demonstrated a quantitative correlation between the FRET signal and the degradation of the HPMA copolymer conjugates. Thus our hypothesis that FRET imaging is suitable for the determination of the degradation and fate of backbone degradable HPMA copolymer conjugates has been validated at the cellular level.

15. SUBJECT TERMS: Key words or phrases identifying major concepts in the report
FRET imaging; biodegradable HPMA copolymer carriers; epirubicin; ovarian cancer; long-circulating nanomedicines; cathepsin B.

16. SECURITY CLASSIFICATION OF:			**17. LIMITATION OF ABSTRACT**	**18. NUMBER OF PAGES**	**19a. NAME OF RESPONSIBLE PERSON**
					USAMRMC
a. REPORT	**b. ABSTRACT**	**c. THIS PAGE**			**19b. TELEPHONE NUMBER** *(include area code)*
U	U	U	UU	21	

W81XWH-13-1-0160

FRET Imaging Trackable Long-Circulating Biodegradable Nanomedicines for Ovarian Carcinoma Therapy

Jindřich Kopeček - PI

TABLE OF CONTENTS

1. INTRODUCTION

The project proposes to develop a new biodegradable polymeric drug delivery system for the treatment of ovarian cancer that is capable of non-invasive assessment of therapeutic efficacy. The evaluation/imaging of this new system is based on Fluorescence (Förster) Resonance Energy Transfer (FRET) fluorescence molecular tomography (FMT) imaging combined with positron emission tomography (PET) imaging. The anticipated outcome of this project is to provide a powerful tool for tracking and screening biodegradable nanomedicines in preclinical evaluation. Moreover, this real-time monitoring technique will permit to gain insight into the structure-efficacy relationship and identify factors impacting effectiveness. Ultimately, optimized polymer-drug conjugates with significant efficacy toward ovarian cancer will be produced.

2. KEYWORDS

FRET imaging; biodegradable HPMA copolymer carriers; epirubicin; ovarian cancer; long-circulating nanomedicines; cathepsin B.

3. OVERALL PROJECT SUMMARY

i. Design and synthesis of FRET pair-labeled biodegradable HPMA copolymer conjugates.

To visualize the degradation process of HPMA copolymer carrier by FRET imaging, two chromophores, one donor and one acceptor, have to be included in the degradable system in less than 10 nm distance. The hydrodynamic radius of polyHPMA is <5 nm when Mw is ≤60 kDa [1]. Therefore, we hypothesized that FRET will occur when one chromophore will tag the HPMA polymer segment, and the other will be inserted via the enzyme-sensitive peptide linker. Additionally, the detachment of one chromophore from the backbone by enzymatic cleavage will result in a loss of FRET effect.

As the first step, we designed and prepared a HPMA copolymer conjugate containing a popular FRET pair Cy3/Cy5 (P-Cy3-Cy5) as shown in **Scheme** 1A using RAFT (reversible addition-fragmentation chain transfer) polymerization [2,3] followed by conjugation of Cy3 and/or Cy5 to the polymer. Here, the donor fluorophore Cy3 was attached to the HPMA copolymer backbone via a cleavable (by lysosomal proteases) tetrapeptide linker GFLG (Gly-Phe-Leu-Gly), while the acceptor Cy5 was directly attached to the HPMA backbone. The free (unbound) dyes were removed by chromatography using an LH20 column with methanol as eluent. Single labeled conjugates (P-Cy3 and P-Cy5) were synthesized (Scheme 1B) and used as controls in FRET investigation.

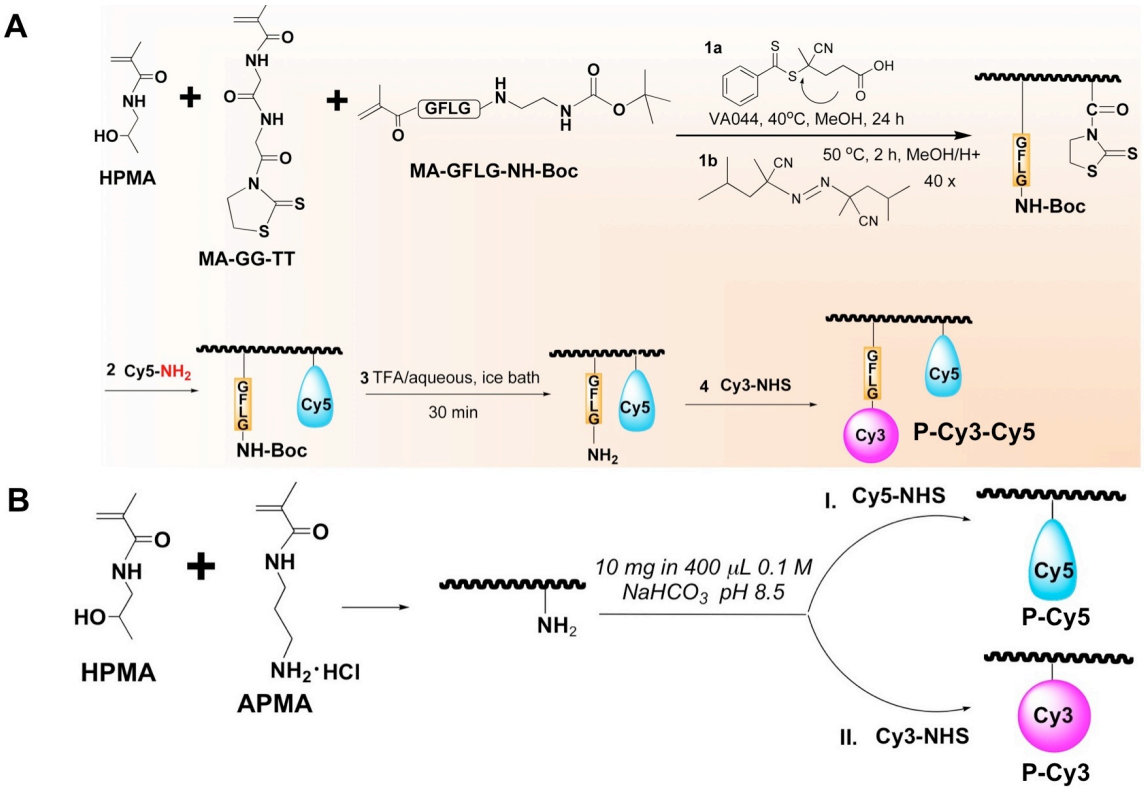

Scheme 1. (A) Synthesis of Cy3/Cy5 dual-labeled HPMA copolymer conjugates P-Cy3-Cy5; (B) Synthesis of Cy3- or Cy5-labeled HPMA copolymer conjugates (controls).

ii. Characterization of FRET pair-labeled biodegradable HPMA copolymer conjugates.

The average molecular weight (Mw) and molecular weight distribution (Mw/Mn) of the polymer conjugates labeled with Cy3 and/or Cy5 were determined with size-exclusion chromatography (SEC) on an AKTA FPLC system (GE Healthcare) equipped with miniDAWN TREOS and OptilabEX detectors (Wyatt Technology, Santa Barbara, CA). UV-vis spectra indicated that the conjugates have identical extinction/emission (Ex/Em) properties compared with the low molecular weight chromophores (Fig. 1 A,B). Therefore the content of labels was determined via UV-vis spectrophotometry (Varian Cary 400) using molecular extinction coefficients of Cy3 and Cy5, respectively. The characterization results are listed in Table 1.

Table 1. Polymer conjugates synthesized for FRET characterization

Samples	Mw (kDa)	Mw/Mn [a]	Content [b], nmol/mg		Ex, nm	Em, nm
			Cy3	Cy5		
P-Cy3	41	1.10	294		548	562
P-Cy5				284	646	664
P-Cy3-Cy5	61	1.09	332	268	520	500-750 [c]

[a] Using Superose 6 HR10/30 column with 0.1 M sodium acetate buffer /30% acetonitrile (v/v) pH 6.5.
[b] Determined in methanol.
[c] Scanned in range of 500-750 nm.

FRET investigation of P-Cy3-Cy5 was conducted by fluorescence spectrophotometry. Wavelength 520 nm was selected for excitation to minimize the contribution of Cy5 emission. As expected, when the conjugate was excited using Ex 520 nm, a significant emission peak of Cy5 was observed in the conjugate P-Cy3-Cy5 but it was not found in the mixture of P-Cy3+P-Cy5 (Fig. 1C). After the conjugate P-Cy3-Cy5 was exposed to papain, a mimic of lysosomal enzyme, the emission peak of Cy5 at 664 nm almost disappeared (Fig. 1C). The loss of FRET signal is due to the enzymatic cleavage of the GFLG linker and consequent release of Cy3 from the polymer backbone. **These results support our hypothesis that FRET can be used as a tool to elucidate the fate of the polymer backbone and of the cleavable drug.**

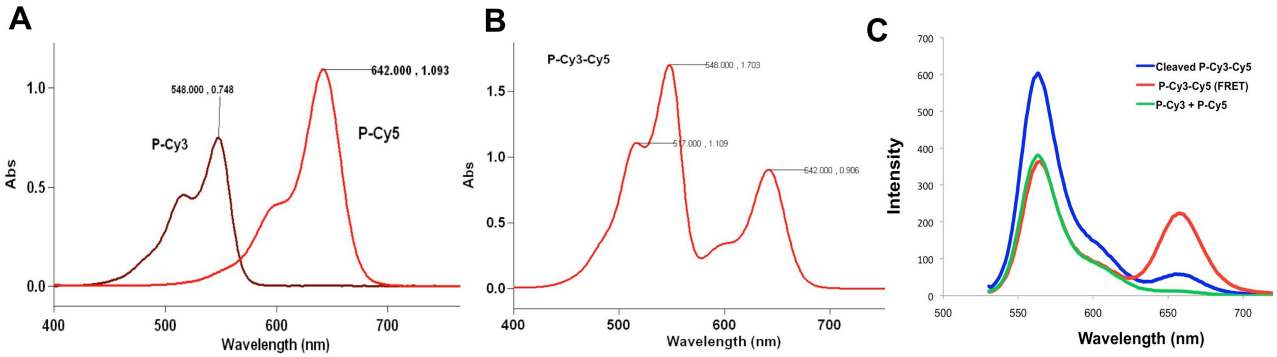

Figure 1. UV spectra of labeled conjugates P-Cy3, P-Cy5 and P-Cy3-Cy5 (A,B); Fluorescence spectra of conjugates P-Cy3-Cy5 before and after cleavage by enzyme (excitation 520 nm) (C).

iii. In vitro evaluation of FRET pair-labeled biodegradable HPMA copolymer conjugates.

The conjugate with FRET feature, P-Cy3-Cy5, was used to further investigate its fate at the cellular level (cleavage and release of payload).

Tumor cells over-express cathepsin B. The oligopeptide GFLG has been identified from detailed studies of cathepsin B specificity and widely used as a lysosomally cleavable linker in polymeric nanomedicines [4]. When the FRET conjugate P-Cy3-Cy5 was incubated with tumor cells, cleavage of the GFLG linker and consequent release of Cy3 from the polymer backbone resulted in loss of FRET signal. Therefore, we chose the human ovarian carcinoma A2780 cell line to investigate the fate of the conjugate P-Cy3-Cy5 by FRET confocal microscopy.

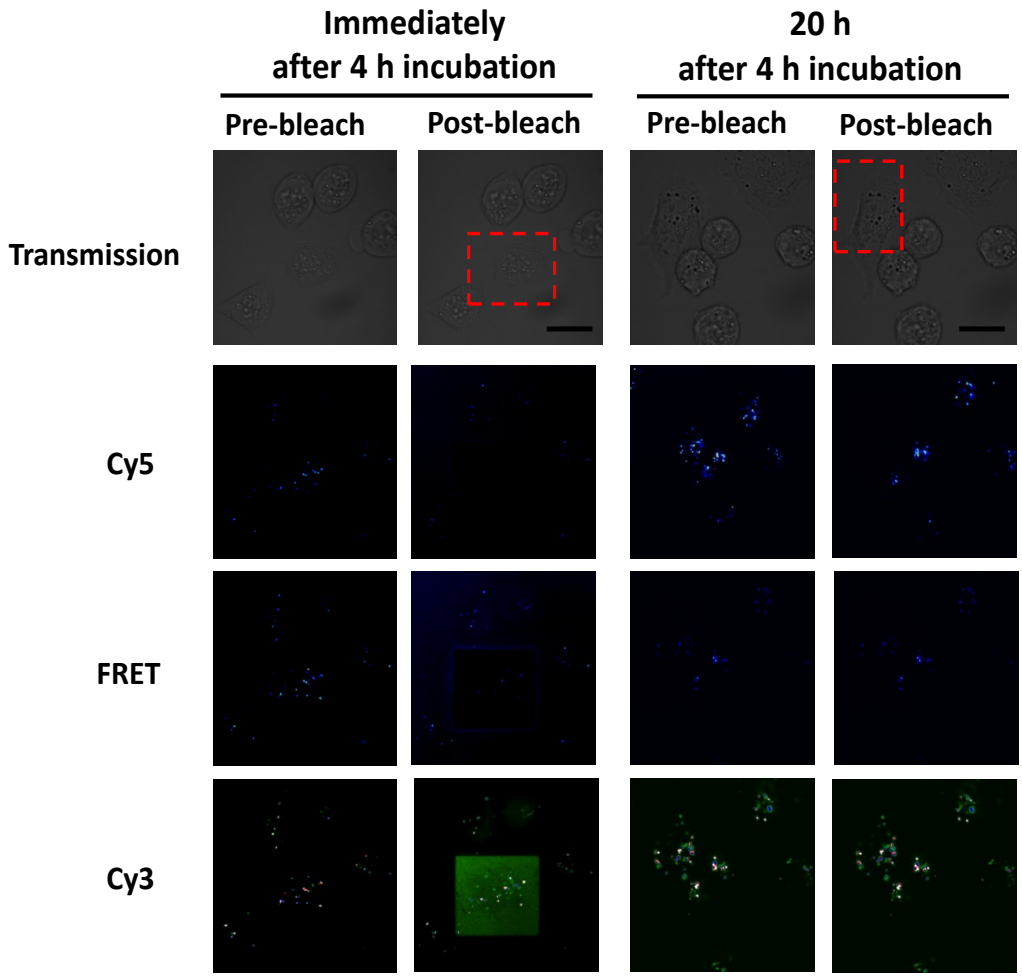

Figure 2. Visualization by FRET of payload Cy3 release from P-Cy3-Cy5 conjugate in cathepsin B over-expressing A2780 human ovarian cancer cells. The cells were first incubated with P-Cy3-Cy5 at 37°C for 4 h and then were washed. Half of the cells were fixed immediately, while the other half were incubated with fresh medium at 37°C for another 20 h and fixed. The fixed cells were observed under confocal microscope using the standard acceptor Cy5 photobleaching method. Bleached regions are indicated by red boxes. Representative pre- and post-bleach images are shown. Scale bar, 10 μm.

Cathepsin B-overexpressing human ovarian cancer A2780 cells were incubated with the FRET conjugate (see caption to Fig. 2). The fixed cells were observed using the standard acceptor Cy5 photobleaching FRET confocal microscopy, which is a more straightforward approach for performing FRET. In this experiment, we collected pre-bleach and post-bleach images. To do the photobleaching, the cells were exposed to high excitation intensity at an excitation wavelength of 646 nm for a 20 min period. After high-energy laser treatment, there was a dramatic reduction of Cy5 intensity in the bleached regions (Fig. 2). In the cells immediately following 4 h incubation, we found that FRET intensity also significantly decreased and bleaching the acceptor Cy5 resulted in any substantial increase in donor Cy3 fluorescence, because the acceptor can no longer receive energy from the donor. However, those intensity changes did not occur in the same batch of cells after additional 20 h culture (Fig. 2). This indicated that the payload Cy3 had been released from the backbone after cellular internalization and lysosomal cleavage.

To confirm the FRET changes over the time, we further investigated the cell lysis using fluorescence spectrophotometry. The ratio, $I_A/(I_D + I_A)$, was calculated to quantify the FRET change, where I_A and I_D are the fluorescence intensities at 662 nm and 564 nm, respectively (excitation 520 nm). In A2780 cancer cells, the ratio decreased to 0.27 at 4 h and gradually decreased to 0.20 at 12 h and 0.14 at 24 h (Fig. 3). Comparing with the ratios in initial stock (0.33) or in medium alone (0.30), our observation suggests an effective release of Cy3 molecules from the conjugate. In the meantime, we also analyzed Cy3 release in NIH/3T3 normal cells. Because cathepsin B activity is extremely low in NIH3T3 cells [5], the ratio only decreased to 0.27 at 24 h (Fig. 3). In summary, our FRET results demonstrated that the release of payload Cy3 is highly dependent on the cathepsin B level. It has been reported that cathepsin B level is much higher in malignant tumors, such as ovarian [6,7], melanoma [8], breast [9], lung [10], stomach [11], and colon [12] tumors, as compared to normal cells. It acts as an important proteinase of matrix materials to degrade surrounding proteins and other tissue components so that cancer cells can invade and metastasize. Therefore, high expression of cathepsin B in tumor cells can induce a fast release of drugs from conjugates and enhance the uptake ratio of tumor to normal tissues, thereby resulting in improved therapeutic efficacy and safety profile.

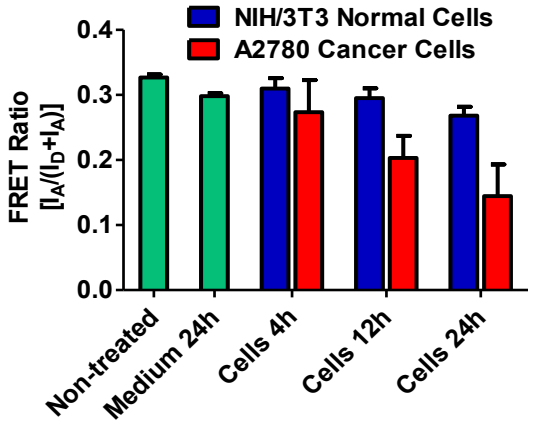

Figure 3. FRET ratios of P-Cy3-Cy5 conjugate in NIH3T3 normal cells (cathepsin B negative) and A2780 ovarian cancer cells (cathepsin B over-expressing) at different intervals. The cells were incubated with P-Cy3-Cy5 at 37°C for 4 h and then were cultured in fresh medium for another 0, 8 or 20 h. Then cell lysis was measured by fluorescence spectrophotometry. FRET ratio = $I_A/ (I_D+I_A)$. I_A and I_D are the fluorescence intensities at 662 nm and 564 nm, respectively (Ex 520 nm).

iv. Design, synthesis and characterization of FRET pair-labeled biodegradable HPMA copolymer-epirubicin conjugates.

Epirubicin has been regarded as one of the most active drugs for cancer patients, particularly those with metastatic disease. It has shown equivalent cytotoxic effects to doxorubicin (DOX) in human ovarian cancer cells, but possesses decreased cardiotoxicity and myelotoxicity than DOX at equimolar doses. In this project, we proposed to use HPMA copolymer-epirubicin conjugates as a "proof-of-concept" model for the development of new macromolecular therapeutics and a new imaging strategy. We synthesized a polymerizable epirubicin derivative (MA-GFLG-EPR, *N*-methacryloylglycylphenylalanylleucylglycyl-epirubicin) and prepared HPMA copolymer-epirubicin conjugates by RAFT copolymerization. Considering the drug inherent fluorescence, we also synthesized Cy5-labeled HPMA copolymer-epirubicin conjugates (P-EPR-co-Cy5) (Scheme 2). We anticipate using FRET as a tool to monitor in real time intracellular release of EPR from the carrier and to gain a detailed insight into the structure-efficacy relationship.

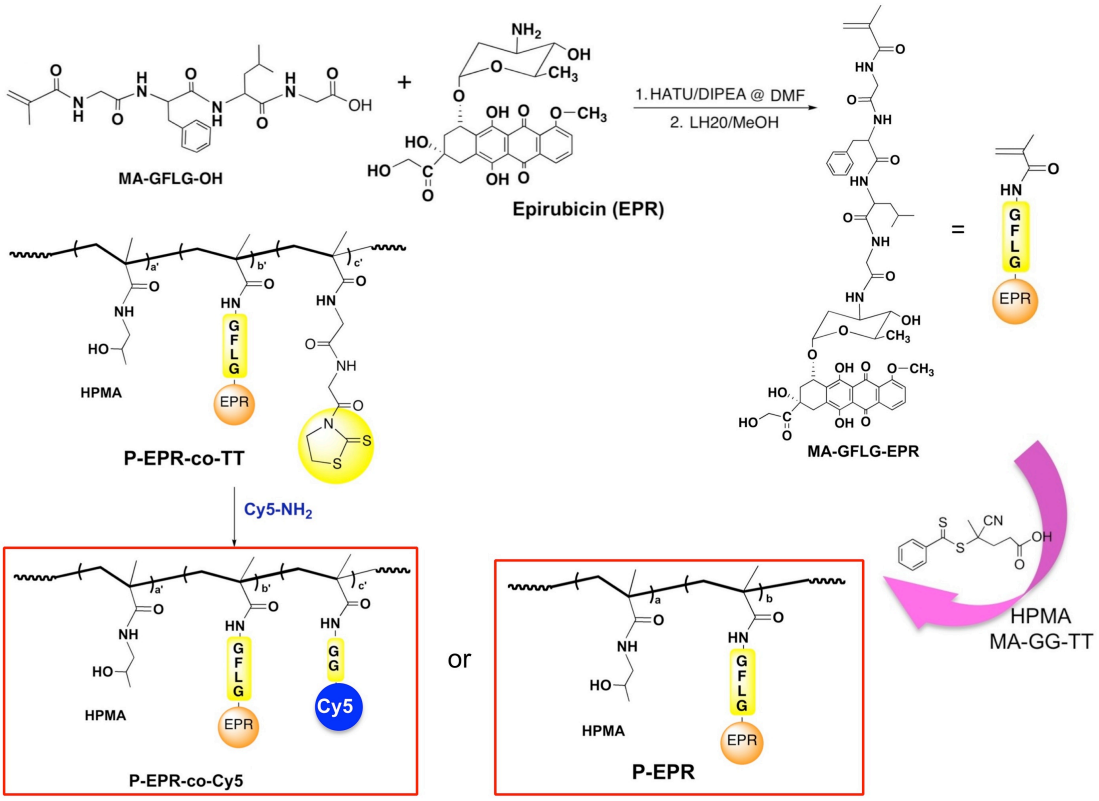

Scheme 2. Synthesis of polymerizable derivative of epirubicin (MA-GFLG-EPR), HPMA copolymer-epirubicin conjugate (P-EPR), and Cy5-labeled HPMA copolymer-epirubicin conjugate P-EPR-co-Cy5.

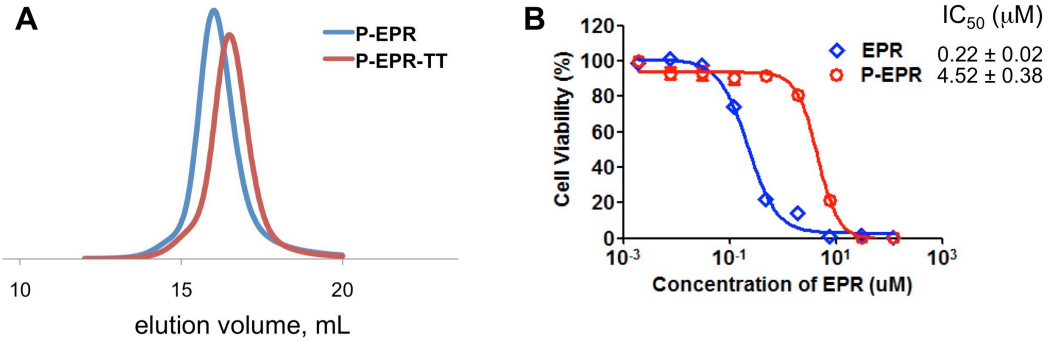

Figure 4. HPMA copolymer-epirubicin conjugate (P-EPR) had cytotoxic potency. (A). SEC profiles of P-EPR and P-EPR-TT. (B). *In vitro* cytotoxicity of free drug epirubicin (EPR) and its HPMA copolymer conjugate (P-EPR) toward A2780 human ovarian carcinoma cells.

The successful synthesis of HPMA copolymer-EPR conjugate was confirmed by composition analysis and SEC profile (Fig. 4A). The cytotoxicity of free drug (EPR) and its HPMA copolymer conjugate (P-EPR) against A2780 human ovarian cancer cells was determined. Cell-growth inhibition curves and IC_{50} values are presented in Fig. 4B. Overall, both EPR and P-EPR showed a dose-dependent cytotoxicity against A2780 cells. The IC_{50} values revealed that HPMA copolymer-EPR conjugate exhibited less cytotoxicity than EPR, which is due to different mechanisms of cell entry - diffusion (free drugs) vs. endocytosis (conjugates). **Importantly, the FRET property was also observed in the conjugate P-EPR-co-Cy5** when using 445 nm as the excitation wavelength (Fig. 5).

Samples	Ex, nm	Em, nm
EPR (P-EPR)	445	560
Cy5 (P-Cy5)	646	664
P-EPR-Cy5	445	325-750

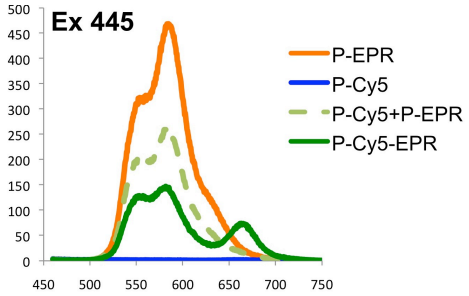

Figure 5. P-EPR-Cy5 showed FRET property. Fluorescence spectra of conjugates (P-EPR-Cy5, P-EPR, P-Cy5, P-EPR+P-Cy5).

v In vivo evaluation of biodegradable HPMA copolymer-epirubicin conjugates.

Tumor Model. All animal studies were carried out in accordance with the University of Utah IACUC guidelines under approved protocols. A2780 human ovarian cancer cells (5 x 10^6) in 100 µL of phosphate buffer saline were subcutaneously inoculated in the right flank of 6- to 8-week-old syngeneic female nude mice (22–25 g, Charles River Laboratories).

The impact of Mw of polymer conjugates on treatment efficacy and elimination rate. We have synthesized the 1st generation of HPMA copolymer-epirubicin conjugate (P-EPR) and 2nd generation biodegradable long-circulating HPMA copolymer-epirubicin conjugate (2P-EPR, 2nd generation conjugate). The targetability of conjugates containing Fab' antibody fragments will also be evaluated. Currently the mice have been inoculated with cancer cells and the conjugates will be administered when the tumor size reaches a proper size. Three-dose administration will be applied. The inhibition of tumor growth, body-weight and metabolism of the conjugates will be closely monitored.

vi Design and synthesis of multiblock FRET pair-labeled biodegradable HPMA copolymer conjugates via RAFT copolymerization followed by azide-alkyne 'click' reaction.

To prove our hypothesis that the cleavage of long-circulating polymer-drug conjugates at specific location will trigger fluorescence signal changes, dual-labeled biodegradable HPMA copolymer conjugates were synthesized in three steps (Scheme 3). In the first step, HPMA and *N*-(3-aminopropyl)methacrylamide (APMA) were copolymerized by the RAFT process using an α,ω-dialkyne trithiocarbonate based chain transfer agent. In the second step, the copolymer was labeled with Cy3 via the reaction of amino groups at side chain termini with Cy3-*N*-hydroxysuccinimide ester (Cy3-NHS). Unreacted dye was removed by chromatography on an LH20 column with methanol as the mobile phase. Successful Cy3 attachment was confirmed via HPLC and degree of labeling was calculated from the absorbance of the polymer stock of known concentration using the molecular weight of the polymer and the extinction coefficient of the dye. Finally, in the third step the polymer chains were extended by the reaction of the α,ω-dialkyne Cy3-labeled polymer (unimer) and the Cy5-labeled chain extender in a Cu(I)-rich aqueous solution to generate multimers with both Cy3 and Cy5 incorporated into the backbone. Unreacted peptide was removed by chromatography on an LH20 column with methanol as the mobile phase. Chain extension was confirmed by comparing the product's size exclusion chromatograph (obtained via AKTA FPLC) against the profile of the constituent unimer. Presence of the Cy5 dye in the polymer was confirmed via analysis of the absorbance spectra and the presence of a distinct peak at 646 (corresponding to the λ_{max} of Cy5) that was not present in the unimer spectra.

The enzymatically-degradable α,ω-diazide chain extender, α,ε-bis(azidophenylglycyl-phenylanalylleucylglycyl)lysine, was synthesized via solid phase peptide synthesis. The intermediate was modified using a bi-functional linker (*N*-Boc ethylenediamine) to create a primary amine functional group that was subsequently reacted with an active NHS-ester of the acceptor fluorophore Cy5. Unreacted dye was removed via HPLC purification. Purity and identity of the final product was confirmed via HPLC and ESI-mass spectrometry, respectively.

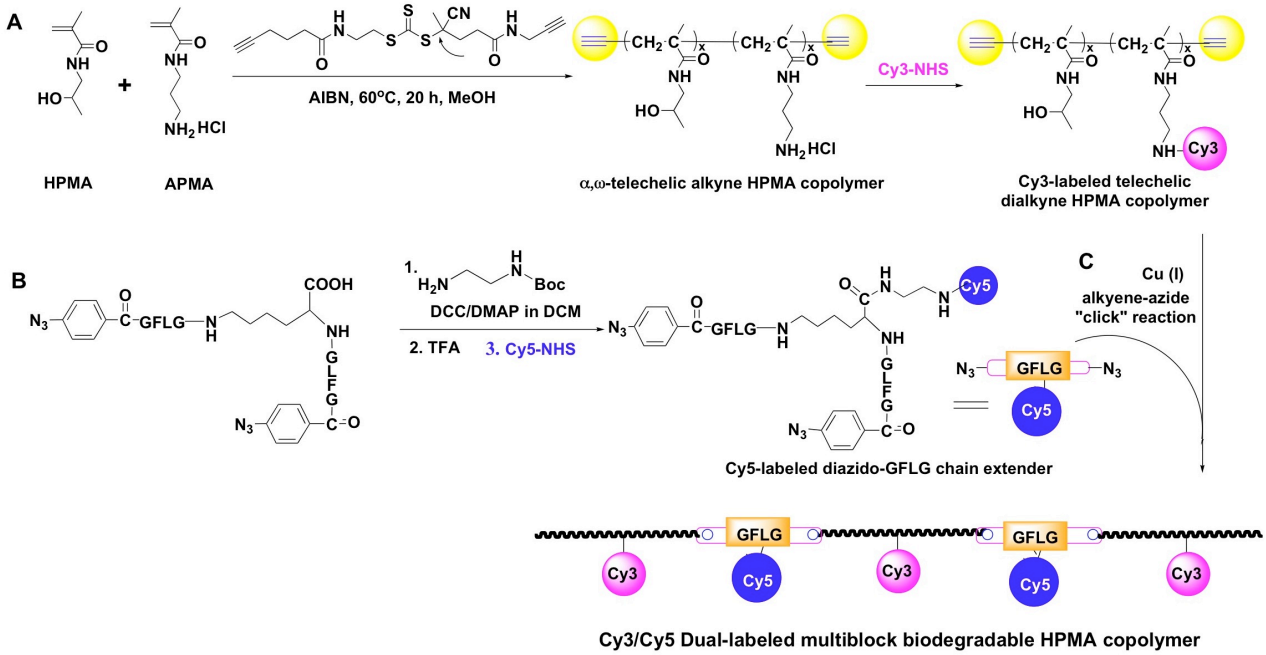

Scheme 3. Synthesis of Cy3/Cy5 dual-labeled biodegradable HPMA copolymer conjugates in three steps: (A) Synthesis of Cy3-labeled HPMA copolymer conjugates; (B) Synthesis of Cy5-labeled enzyme-cleavable chain extender; (C) Cu (I)-assisted azide-alkyne click reaction.

vii. Confirmation of successful fluorescence resonance energy transfer as a property of chain extension.

The fluorescence profile of the dual-labeled chain extended backbone degradable multimer was analyzed (using a Tecan Infinite M1000 PRO Microplate Spectrophotometer) and compared against the fluorescence profile of its two components (the Cy3-labeled unimer and the Cy5-labeled chain extender). Three channels (Table 2), each consisting of a single excitation and emission wavelength pair, were analyzed.

Table 2: Summary of Fluorescence Channels used for Analysis

Channel Name	Interpretation	Ex, nm	Em, nm
Cy3 Channel	Emission from the Cy3 dye resulting from its direct excitation	546	567
Cy5 Channel	Emission from the Cy5 dye resulting from its direct excitation	646	669
FRET Channel	Emission from the Cy5 dye arising from direct excitation of Cy3 followed by nonradiative energy transfer to Cy5	546	669

When controlling for the intensity in the Cy3 channel, the emission in the FRET channel was significantly greater than could be accounted for by the simple sum of the two components. Furthermore, mixing the two components in a copper-free solution at similar concentration (as determined by absorbance at 546 and 646) did not give rise to an equivalent FRET channel intensity (Fig. 6). Therefore, this phenomenon is an emergent property of successful chain extension and the resulting proximity of the dye pair.

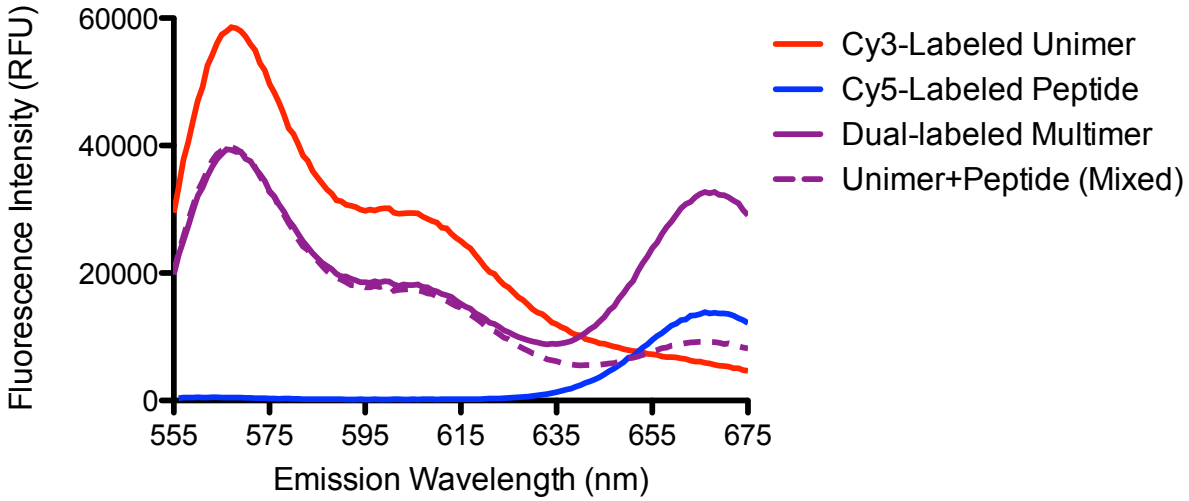

Figure 6. Comparison of fluorescence emission profile for the single labeled conjugates, a mixture of two conjugates, and the clicked multiblock conjugate. All samples were excited at 546 nm.

Furthermore, upon exposure to an 8 μM papain solution for 2 h, the emission in the FRET channel is significantly reduced and the fluorescence profile converges back to that of the constituent Cy3-labeled unimers (Fig. 7). This indicates that the energy transfer between the Cy3 and Cy5 dye is severed upon enzymatic cleavage of the backbone.

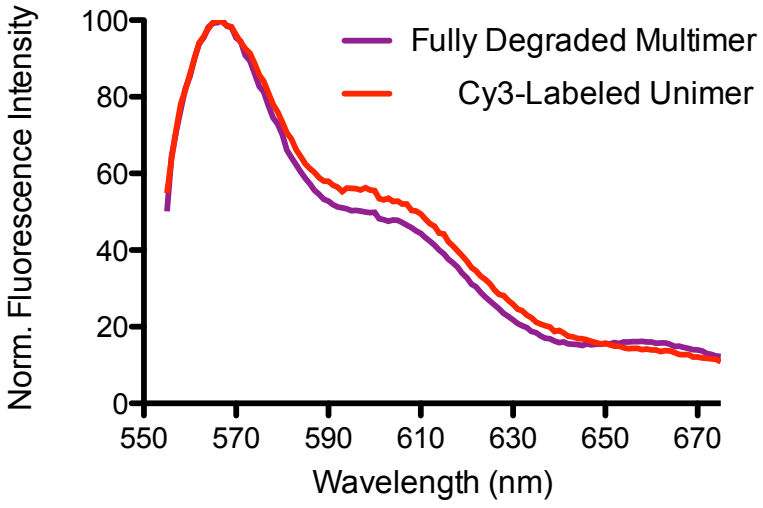

Figure 7. Comparison of fluorescence emission profiles for Cy3-labeled unimer and fully degraded dual-labeled multimer (exposed to 8 μM papain solution for 2 h). Both samples were excited at 646 nm and emission was measured from 555 to 675 nm.

viii. Establishment of a quantitative relationship between degree of backbone degradation and intensity of the fluorescence signal.

To establish a quantitative relationship between intensity of the fluorescence signal and the structure of polymer conjugates, a set of dual-labeled biodegradable clicked products with various degrees of backbone degradation were prepared and analyzed. In brief, the dual-labeled biodegradable clicked product (3 mg/mL) was incubated in a 0.08 μM papain solution. At predetermined time points, a sample was withdrawn from the reaction and added to an inhibitor solution (100 μM iodoacetic acid sodium salt in methanol acidified with 0.02% v/v acetic acid) to inactivate the enzyme.

Analysis of the three fluorescence channels (Table 2) indicated that greater incubation resulted in decreased emission in the FRET and Cy5 channels as well as increased emission in the Cy3 channel. The trends in the FRET and Cy3 channels are consistent with a loss of energy transfer, as the acceptor will no longer fluorescence without a nearby donor (thereby decreasing its fluorescence) and the donor will no longer be quenched by the interaction (thereby increasing its fluorescence). These trends can be observed in Figures 8 and 9.

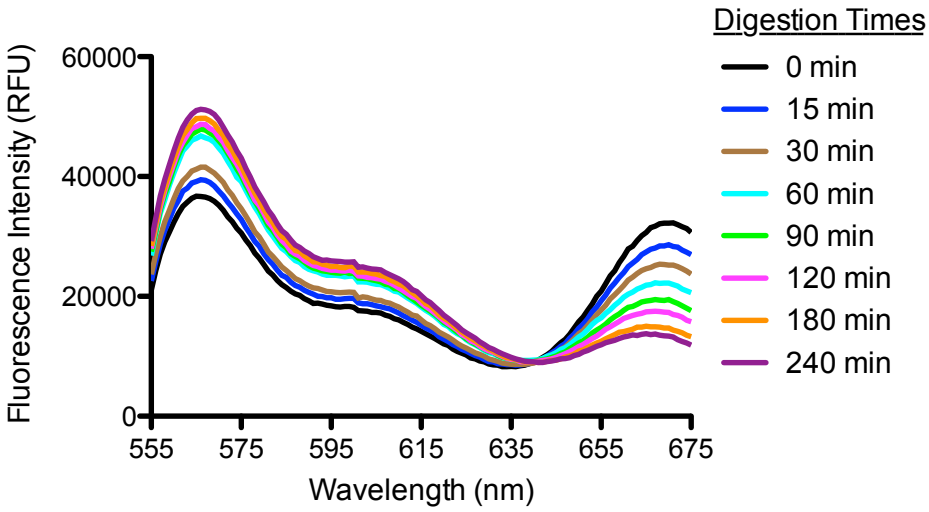

Figure 8. Evolution of fluorescence emission profile over the course of degradation. Times correspond to length of incubation with 0.08 μM of papain before inhibition. All profiles are the result of excitation at 546 nm and measurement of the emission from 555 to 675 nm.

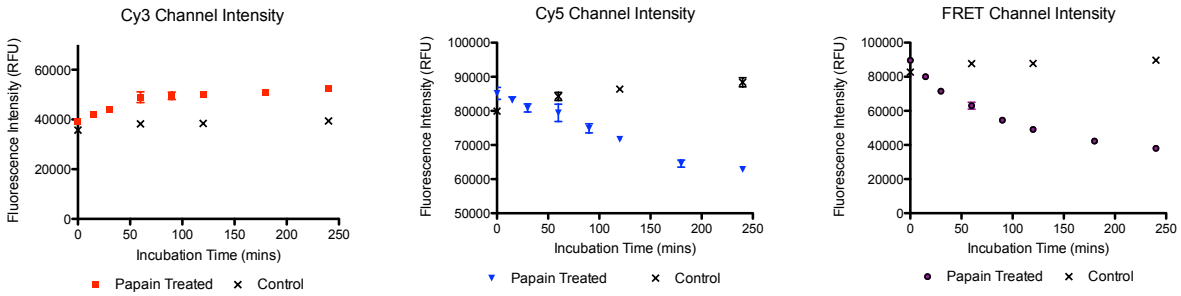

Figure 9. Fluorescence intensity in each channel as a function of incubation time with papain. Controls were incubated in identical buffer conditions without enzyme present. Each point corresponds to the mean of three samples, each taken from a different stock. Error bars indicate standard error of the mean. Each channel was measured independently.

The decrease of fluorescence intensity in the Cy5 channel over time is likely the result of a difference in quantum yield of the Cy5 dye when incorporated into the polymer backbone versus free peptide. This is also supported by the observed shift in the Cy5 emission maxima from 669 to 664 nm upon cleavage and release of the free peptide.

Small variations in the sample concentration were accounted for by normalizing the FRET channel intensity to the sample's Cy3 channel emission (Fig. 10).

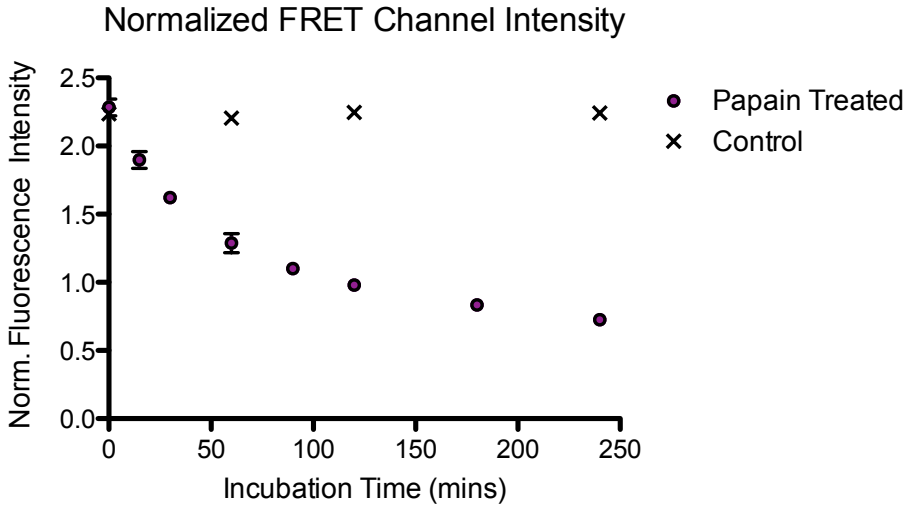

Figure 10. Ratio of FRET channel and Cy3 channel emissions as a function of incubation time with papain. Controls were incubated in identical buffer conditions without enzyme present. Each point corresponds to the mean of three samples, each taken from a different stock. Error bars indicate standard error of the mean.

In addition, the size exclusion chromatograph of a sample at each time point was analyzed via the AKTA FPLC system [UV detection at 280nm]. Longer digestion times resulted in an increase in lower molecular weight polymers, represented by higher signal intensity at higher elution volumes (Fig. 11).

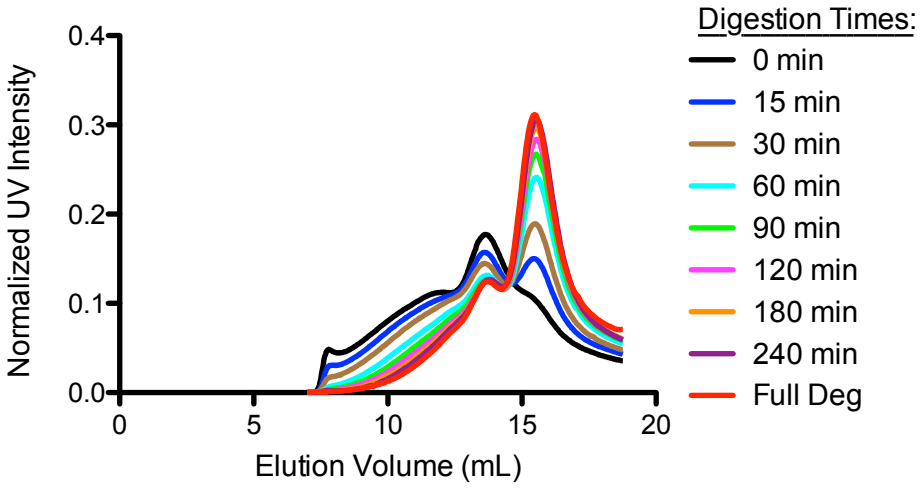

Figure 11. SEC profiles as a function of incubation time with papain. Profiles obtained by measuring absorbance of elutant at 280 nm. Fully degraded sample was obtained by exposing polymer to an 8 μM papain solution for two hours.

In order to quantify the extent of degradation at each time point, a “percent conversion” metric for each SEC profile was calculated by comparing the degree of this rightward shift in the chromatograph with the profile for undigested multimer (set to 0% conversion) and a fully degraded sample (set to 100% conversion).

Specifically, each SEC profile was normalized to give each curve an AUC (area under the curve) of 1, then compared to the area-normalized profile on an undigested multimer sample. The fraction of area that did not overlap between the curves (i.e. the fraction shifted to higher elution volumes) was taken to correlate with extent of degradation. These fractions were then normalized by the value for the fully digested sample to generate a value for percent conversion. An example of this process is provided in Figure 12.

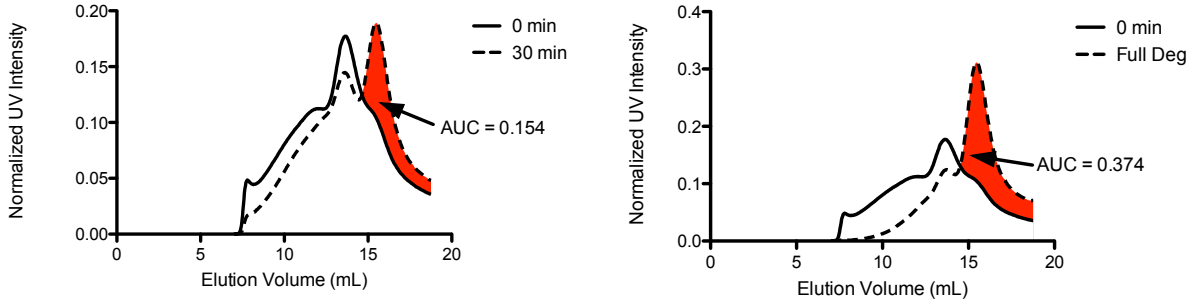

Figure 12. Demonstration for quantifying “percent conversion” from SEC profiles. Times correspond to duration of exposure of papain. The area in red represents the percent mass that has shifted to later elution times as a result of degradation. Upon full degradation, this area has grown to a value of 0.374, which is taken to represent 100% conversion. Therefore, an area of 0.154 (as shown at 30 min time point above) would represent 41.2% conversion.

Furthermore, this percent conversion was accurately tracked by changes in the fluorescence spectra of the system. The ratio of emission intensities in the FRET and Cy3 channels could be mapped onto the percent conversion metric to generate a linear relationship between the two measurements (Fig. 13). Therefore, degree of FRET accurately not only reflects but also quantitates the extent of degradation of this multimer construct, allowing for polymer state to be accurately predicted using only fluorescence data.

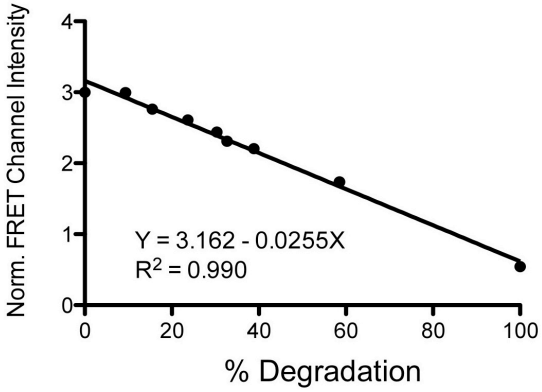

Figure 13. FRET channel intensity (normalized to Cy3 channel intensity) plotted against the extent of degradation values calculated from the SEC profiles. These two sets of values, despite being obtained from entirely different techniques, show strong linear correlation with one another. Normalized FRET channel intensity is represented as the mean of three samples, each taken from a different stock. Error bars indicate standard error of the mean. Percent degradation (conversion) was calculated from shifts in SEC chromatographs between representative profiles from each time point.

4. KEY RESEARCH ACCOMPLISHMENTS

- Validation of hypothesis that FRET imaging is suitable for the determination of the degradation and fate of backbone degradable HPMA copolymer conjugates.
- A technique that quantitatively relates degree of FRET with extent of degradation is generally applicable for polymer-based nanomedicines.
- Novel synthetic procedures combining RAFT polymerization and click (azide-alkyne) reactions contributed to the development of bioconjugate chemistry.
- Correlation of the FRET signal on one hand with the level of cathepsin B expression and with the intracellular degradation of the conjugates on the other hand.
- Epirubicin can be used as a donor in FRET during in vitro evaluation of the degradability of bioconjugates.

5. CONCLUSION

The major goal of the proposed project is to develop a novel FRET imaging strategy, which permits visualizing the biodegradation of copolymer-drug conjugates at the body, tissue and cell levels in real time. The information will initiate our understanding of *in vivo* behavior of biodegradable polymers and help to shape the design of highly efficient and less toxic delivery systems. In addition to drug delivery, biodegradable polymers are also widely used for gene transfer, tissue engineering, and regenerative medicine. We anticipate that the success of this project will accelerate the translation of numbers of biodegradable polymers from bench to clinic and ultimately spark a breakthrough for the treatment of ovarian cancer and other diseases.

In the first year of the project we have synthesized numerous FRET trackable biodegradable HPMA copolymer conjugates that were labeled with Cy3 and/or Cy5, conjugates that contain epirubicin and performed click reactions for chain extension to manipulate the molecular weight of the biodegradable conjugates. The conjugates were characterized by physicochemical methods and in vitro using human ovarian carcinoma cells. FRET technique was used to investigate the conjugates at cellular level. We achieved correlation of the FRET signal on one hand with the level of cathepsin B expression and with the intracellular degradation of the conjugates on the other hand. In fluorescence spectrophotometry experiments we have demonstrated a quantitative correlation between the FRET signal and the degradation of the HPMA copolymer conjugates. Thus it appears that our hypothesis that FRET imaging is suitable for the determination of the degradation and fate of backbone degradable HPMA copolymer conjugates has been validated.

Future plans:

We shall expand the number of cell lines used and determine the backbone degradation and drug release using immunostaining, confocal fluorescence microscopy, and other fluorescence techniques.

Compare kinetics of epirubicin release from the conjugates by cathepsin B with papain (done).

We have initiated in vivo experiments and will continue the in vivo evaluation with the ultimate aim to achieve a positive in vitro – in vivo correlation/validation. The in vivo experiments will include FRET and SPECT/CT imaging (to separately monitor the fate of the carrier (distribution and degradation), release of the drug from carrier, and drug location), biodistribution and pharmacokinetic studies, determination of the maximum tolerated dose, comparison of Fab' fragment targeted and non-targeted conjugates, and determination of the efficacy of the conjugates in the treatment of experimental cancer.

To support the above studies numerous FRET-trackable (containing AF700/AF750 labeled conjugates), backbone degradable HPMA copolymer-epirubicin conjugates will be synthesized.

6. PUBLICATIONS, ABSTRACTS, AND PRESENTATIONS

a1. Lay Press: Nothing to report

a2. Peer-Reviewed Scientific Journals:

Two manuscripts are in preparation;

a3. Invited Articles: Nothing to report.

a4. Abstracts:

J. Yang, R. Zhang, D.C. Radford, J. Kopeček, Design and Synthesis of FRET-Trackable HPMA-Based Biodegradable Conjugates for Drug/Gene Delivery. 3rd Symposium on Innovative Polymers for Controlled Delivery (SIPCD 2014), Suzhou, China, September 16-19, 2014. Proceedings, p. 145.

D.C. Radford, J. Yang, R. Zhang, J. Kopeček, Quantification of Polymer Backbone Degradation Using Fluorescence Resonance Energy Transfer. NanoUtah 2014 Conference, Grand America Hotel, Salt Lake City, Utah, October 12-15, 2014. Proceedings.

b. Presentations:
Both abstracts listed in a4 are presented at international conferences.

7. INVENTIONS, PATENTS AND LICENSES

Nothing to report.

8. REPORTABLE OUTCOMES

Nothing to report.

9. OTHER ACHIEVEMENTS

Nothing to report.

10. REFERENCES

1. Yang J, Kopeček J (2014) Macromolecular therapeutics. *J Controlled Release* 190:288-303. PMCID: PMC4142088
2. Sadekar S, Ray A, Janát-Amsbury M, Peterson CM, Ghandehari H (2011) Comparative biodistribution of PAMAM dendrimers and HPMA copolymers in ovarian-tumor-bearing mice. *Biomacromolecules* 12:88-96.

3. Yang J, Luo K, Pan H, Kopečková P, Kopeček J (2011) Synthesis of biodegradable multiblock copolymers by click coupling of RAFT-generated heterotelechelic polyHPMA conjugates. *Reactive Functional Polym* 71:294-302. PMCID: PMC3076950
4. Zhang R, Yang J, Sima M, Zhou Y, Kopeček J (2014) Sequential combination therapy of ovarian cancer with degradable *N*-(2-hydroxypropyl)methacrylamide copolymer paclitaxel and gemcitabine cConjugates. *Proc Natl Acad Sci USA* 111(33):12181-12186.
5. Yoshii H, Kamiyama H, Minematsu K, Goto K, Mizota T, Oishi K, Katunuma N, Yamamoto N, Kubo Y (2009) Cathepsin L is required for ecotropic murine leukemia virus infection in NIH3T3 cells. *Virology* 394(2):227-234.
6. Downs LS Jr, Lima PH, Bliss RL, Blomquist CH (2005) Cathepsins B and D activity and activity ratios in normal ovaries, benign ovarian neoplasms, and epithelial ovarian cancer. *J Soc Gynecol Investig* 12(7):539-544.
7. Nishikawa H*,* Ozaki Y, Nakanishi T, Blomgren K, Tada T, Arakawa A, Suzumori K. (2004) The role of cathepsin B and cystatin C in the mechanisms of invasion by ovarian cancer. *Gynecol Onco*l 92(3):881-886.
8. Sloane BF, Dunn JR, Honn KV (1981) Lysosomal cathepsin B: correlation with metastatic potential. *Science* 212(4499):1151-1153.
9. Lah TT, Calaf G, Kalman E, Shinde BG, Russo J, Jarosz D, Zabrecky J, Somers R, Daskal I (1995) Cathepsins D, B and L in breast carcinoma and in transformed human breast epithelial cells (HBEC). *Biol Chem Hoppe Seyler* 376(6):357-363.
10. Ebert W, Knoch H, Werle B, Trefz G, Muley T, Spiess E (1994) Prognostic value of increased lung tumor tissue cathepsin B. *Anticancer Res* 14(3A):895-899.
11. Chung SM, Kawai K (1990) Protease activities in gastric cancer tissues. *Clin Chim Acta* 189(2):205-210.
12. Adenis A, Huet G, Zerimech F, Hecquet B, Balduyck M, Peyrat JP (1995) Cathepsin B, L, and D activities in colorectal carcinomas: relationship with clinico-pathological parameters. *Cancer Lett* 96(2):267-275.

11. APPENDICES

1. Jiyuan Yang, Rui Zhang, D. Christopher Radford, Jindřich Kopeček, (2014) Design and Synthesis of FRET-Trackable HPMA-Based Biodegradable Conjugates for Drug/Gene Delivery, Abstract – 3rd Symposium on Innovative Polymers for Controlled Delivery (SIPCD), Suzhou, China, September 16-19, 2014.
2. Jiyuan Yang, Rui Zhang, D. Christopher Radford, Jindřich Kopeček, (2014) Design and Synthesis of FRET-Trackable HPMA-Based Biodegradable Conjugates for Drug/Gene Delivery, Poster – 3rd Symposium on Innovative Polymers for Controlled Delivery (SIPCD), Suzhou, China, September 16-19, 2014.
3. D. Christopher Radford, Jiyuan Yang, Rui Zhang, Jindřich Kopeček (2014) Quantification of Polymer Backbone Degradation using Fluorescence Resonance Energy Transfer, Abstract – nanoUtah 2014 Symposium, Salt Lake City, UT, October 13-15, 2014.

Design and Synthesis of FRET-Trackable HPMA-Based Biodegradable Conjugates for Drug/Gene Delivery

Jiyuan Yang[1], Rui Zhang[1], D. Christopher Radford[2], and Jindřich Kopeček[1,2]

[1]Department of Pharmaceutics and Pharmaceutical Chemistry, [2]Department of Bioengineering, University of Utah, Salt Lake City, Utah 84112, USA. E-mail: janeyang390@gmail.com

The introduction of degradable oligopeptide sequences into the backbone of *N*-(2-hydroxypropyl)methacrylamide (HPMA) copolymer–drug conjugates resulted in prolonged circulation time and increased tumor to tissue ratio [1]. In order to independently evaluate the fate of the polymer backbone and the drug (epirubicin) we prepared conjugates double-labeled with a FRET pair — the polymer backbone was labeled with Cy5 (via an enzymatically non-cleavable bond), whereas the oligopeptide side-chains were terminated either in Cy3 (drug model) or epirubicin (EPR). Upon enzymatic cleavage of EPR or Cy3 the FRET signal receded. The emission spectra of the conjugates before and after incubation with enzyme solution were measured with an LS 55 Luminescence Spectrometer (Perkin Elmer) (Fig.1 insert). The internalization of the conjugate and drug release at the single A2780 cell level were visualized using a 3D super-resolution Vutara SR-200 fluorescence microscope.

Another design of HPMA copolymers is the dynamic conjugates for the delivery of siRNA/ miRNA. The copolymer carrier is composed of HPMA, *N*-(2-(2-pyridyldithio)ethyl)methacylamide (PDTEMA), *N*-butylmethacrylamide, and *N*-(3-aminopropyl)methacrylamide (APMA). The amino group of APMA serves for reversible modification with semitelechelic (ST) polyHPMA via a pH-sensitive bond based on 2-propionic-3-methylmaleic anhydride (CDM). A thiol-disulfide exchange reaction was used to bind miRNA to PDTEMA side chains via reducible disulfide bonds. Upon internalization and destabilization of the endosomal membrane the reductive environment cleaves covalently bound RNA from the carrier with ultimate localization in the cytoplasm [2]. Both polymer carriers and ST-polyHPMA were synthesized by RAFT (co)polymerization followed by post-polymerization end-modification, and labeled with Cy5/Cy3, respectively. Conjugation of miRNA and its release were confirmed by agarose gel electrophoresis.

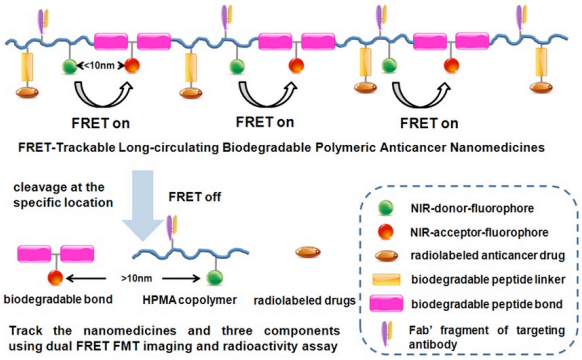

Figure 1. Rationale of the simultaneous tracking of the fate of the carrier and drug by FRET and nuclear imaging.

Key Words: Backbone degradable HPMA copolymers, FRET, RNA, drug delivery.

Acknowledgements: The research was supported in part by US Department of Defense grant W81XWH-13-1-0160.

References

[1] J. Yang, J. Kopeček, Macromolecular therapeutics, J. Control. Release (2014), http://dx.doi.org /10.1016/j/jconrel2014.04013.

[2] B.B. Lundy, A. Convertine, M. Miteva, P.S. Stayton, Neutral polymeric micelles for RNA delivery, Bioconjugate Chem. 24 (2013) 398-407.

Design and Synthesis of FRET-Trackable HPMA-Based Biodegradable Conjugates for Drug/Gene Delivery

Jiyuan Yang[1], Rui Zhang[1], D. Christopher Radford[2], and Jindřich Kopeček[1,2]

Departments of [1]Pharmaceutics and Pharmaceutical Chemistry/CCCD and [2]Bioengineering,
University of Utah, Salt Lake City, Utah 84112, USA

SIPCD III Sep 16-19, 2014
Suzhou, China

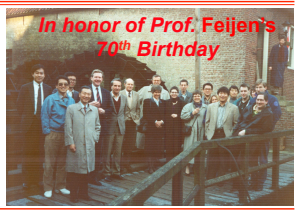

INTRODUCTION

Recently we designed 2nd generation backbone-degradable *N*-(2-hydroxypropyl)methacrylamide (HPMA) copolymer carriers.[1] The combination therapy of A2780 human ovarian carcinoma xenografts with long-circulating HPMA copolymer-paclitaxel/gemcitabine conjugates showed distinct advantages over 1st generation conjugates (Fig. 1A).[2] We used fluorescence resonance energy transfer (FRET) as a tool to track chain scission of the conjugates and to elucidate the fate of the polymer backbone and the drug, respectively (Fig. 1B). Herein we report a rational design and synthesis of conjugates double-labeled with a pair of fluorophores: the polymer backbone was labeled with Cy5, whereas the enzyme-cleavable linker was labeled with Cy3 as drug model or with epirubicin (EPR).

Another application of the FRET technique in our studies was to visualize at cellular level the fate of the HPMA copolymer-based endosomolytic carrier that we developed for delivery of miRNA (Fig.2).

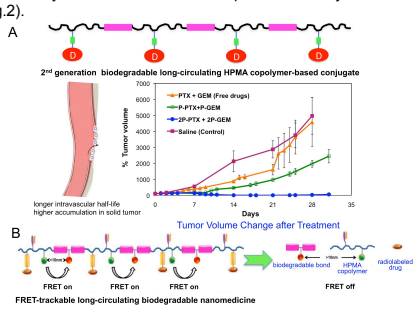

Figure 1. (A) Sequential combination therapy of ovarian cancer with degradable HPMA copolymer paclitaxel (PTX) and gemcitabine (GEM) conjugates. (B) Illustration of simultaneous tracking of the fate of the carrier and drug by FRET and nuclear imaging

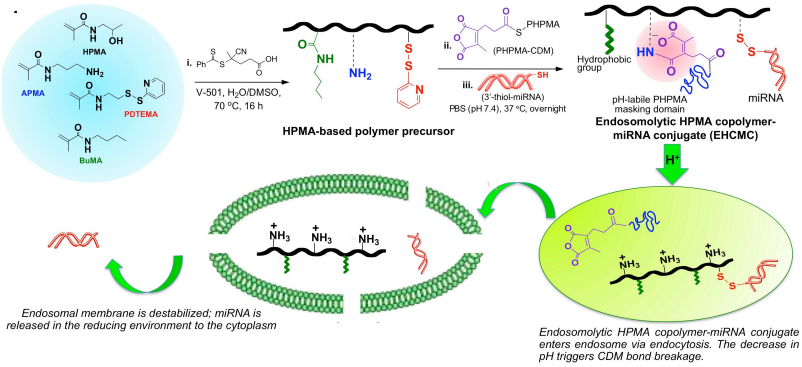

Figure 2. Rational design, synthesis and mechanism of endosomolytic nanomedicines for siRNA/miRNA delivery

EXPERIMENTAL

Synthesis of a FRET nanoprobe conjugate for drug release tracking (P-Cy3-Cy5)

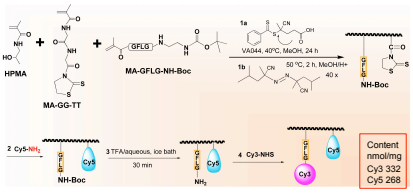

As control, P-Cy5 and P-Cy3 were synthesized:

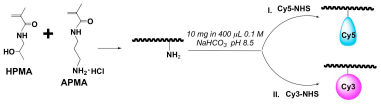

Synthesis of HPMA copolymer-epirubicin (EPR) conjugate

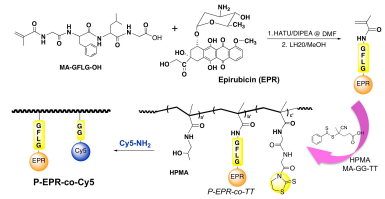

Synthesis of amino-reactive acid-labile semitelechelic polyHPMA

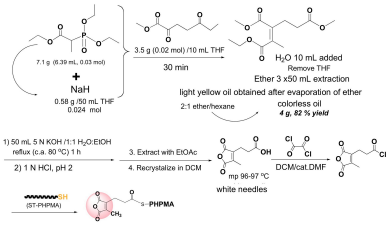

RESULTS

In vitro FRET study of P-Cy3-Cy5

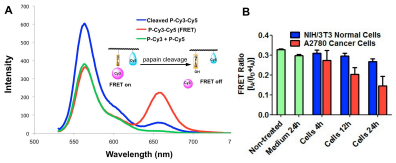

Figure 3. Fluorescence spectra and FRET ratios of conjugate P-Cy3-Cy5 revealed effective payload release following enzyme exposure. (A). Fluorescence spectra of conjugate P-Cy3-Cy5 before or after cleavage by papain (excitation 520 nm). (B). FRET ratios of P-Cy3-Cy5 in NIH3T3 normal cells (low cathepsin B expression) and A2780 ovarian cancer cells (high cathepsin B expression) at different time intervals. The cells were incubated with P-Cy3-Cy5 at 37°C for 4 h and then cultured in fresh medium for another 0, 8, or 20 h. Then cell lysis was measured by fluorescence spectroscopy. FRET ratio = IA / (IA+ID). IA and ID are the fluorescence intensity at 662 nm and 564 nm, respectively (excitation 520nm).

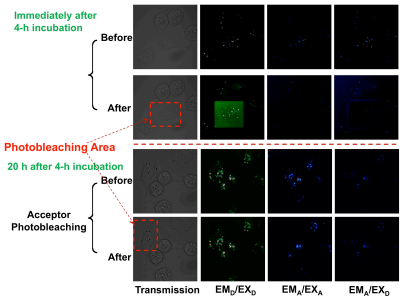

Figure 4. Visualization of payload Cy3 release from conjugate P-Cy3-Cy5 in cathepsin B over-expressing A2780 human ovarian cancer cells by FRET. The cells were first incubated with P-Cy3-Cy5 at 37°C for 4 h and then were washed. Half of the cells were fixed immediately, while the other half were incubated with fresh medium at 37°C for another 20 h and fixed. The fixed cells were observed under confocal microscope using the standard acceptor Cy5 photobleaching method. Bleached areas are indicated by red boxes. Representative images of pre- and post-bleaching are shown.

Evaluation of HPMA copolymer-EPR conjugates

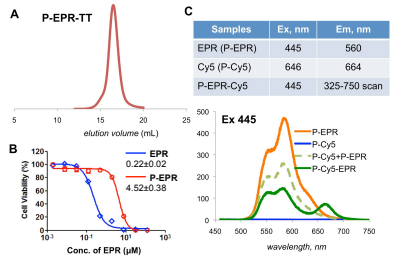

C	Samples	Ex, nm	Em, nm
	EPR (P-EPR)	445	560
	Cy5 (P-Cy5)	646	664
	P-EPR-Cy5	445	325-750 scan

Figure 5. Conjugate P-epirubicin (P-EPR) had cytotoxic potency and its Cy5-labeled derivative showed FRET effect. (A). SEC profile of P-EPR-TT. (B). *In vitro* cytotoxicity of free drug epirubicin (EPR) and its HPMA copolymer conjugate (P-EPR) toward A2780 human ovarian carcinoma cells. (C). Fluorescence spectra of conjugates (P-EPR-Cy5, P-EPR, P-Cy5, P-EPR+P-Cy5).

Validation of reversible attachment of miRNA and pH-dependent destabilization of cell membranes

Table 1. Characterization of polymer precursors

	Mn, Da	PDI Mw/Mn	Yield %	Composition of polymer		
				BuMA	*NH_2*	*PDTEMA*
P-NH_2	63700	1.12	86		3.8% (17 NH_2/chain)	
P-BuMA-NH_2-PDTEMA	48800	1.27	70	~ 30% (molar ratio)	18 NH_2/chain	16 S-S/chain
ST-PHPMA	4800	1.12	98			

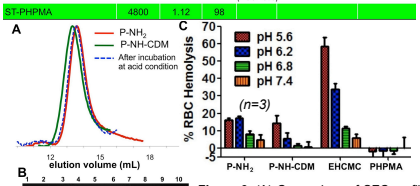

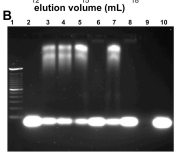

Figure 6. (A) Comparison of SEC profiles of P-NH_2 before and after amino-masking (P-NH-CDM), and after incubation of P-NH-CDM at acidic condition. (B) Gel retardation assay of HPMA copolymer-miR34a conjugates containing a reducible disulfide bond: free miRNA (lanes 2,10); HPMA copolymer-miRNA conjugate (lanes 3,4 with 5x excess, and lanes 5,7 with 10x excess). The bottom shows unbound fraction of miRNA; after addition of 0.1 M DTT to the polymer-miRNA conjugates at 37°C for 30 min (lanes 6,8); polymer only (lane 9) and Mw ladder (lane 1). C). Red blood cell hemolysis assay [3]. Human erythrocytes were incubated with endosomolytic copolymers in a series of buffers simulating the pH range from endosomes (5.6) to physiologic (7.4).

Design & synthesis of FRET-trackable biodegradable HPMA copolymer-based conjugates

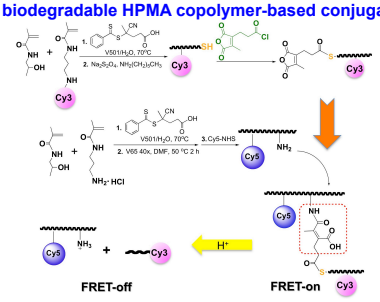

CONCLUSIONS

- We successfully developed dual-labeled conjugates that permit using FRET to monitor drug release and backbone degradation;
- A FRET-trackable dynamic endosomolytic polymer carrier was designed and synthesized. The structure optimization aided by FRET technique is in process.

REFERENCES

1. J. Yang, J. Kopeček, J. Controlled Release 190 (2014) 288-303.
2. R. Zhang, J. Yang, M. Sima, Y. Zhou, J. Kopeček, Proc. Natl. Acad. Sci. USA 111 (2014) 12181-12186.
3. B.B. Lundy, A. Convertine, M. Miteva, P.S. Stayton, Bioconjugate Chem. 24 (2013) 398-407.

ACKNOWLEDGEMENTS

The research was supported in part by US Department of Defense grant W81XWH-13-1-0160. We also acknowledge support in conjunction with grant P30 CA042014 awarded to the Huntsman Cancer Institute, University of Utah.

Postdoctoral position available!

Please visit our website: www.pharmacy.utah.edu/pharmaceutics/groups/kopecek

"Quantification of Polymer Backbone Degradation using Fluorescence Resonance Energy Transfer"

Preferred Session: Emerging Technologies in Biomedical Healthcare: Healthcare and biomedical and emerging technology

Presenter: **D. Christopher Radford,** University of Utah, Department of Bioengineering

Jiyuan Yang[1], Rui Zhang[1], Jindřich Kopeček [1,2]
[1] University of Utah, Department of Pharmaceutics and Pharmaceutical Chemistry/CCCD
[2] University of Utah, Department of Bioengineering

Nanomedicine has great potential to improve the treatment of diseases such as cancer, while minimizing off-target effects. Ideal clinical nanocarriers should specifically accumulate and deliver their payload at the disease site in the short term and eventually be cleared from the body, thus avoiding chronic biocompatibility concerns.

Towards this end, we have previously developed long-circulating backbone-degradable *N*-(2-hydroxypropyl)methacrylamide (HPMA) copolymers. Individual macromolecules with sizes below the renal clearance threshold were chained into high molecular weight multimers bridged by lysosomally-degradable linkers. Upon endocytosis, these linkers would be cleaved, regenerating the low molecular weight polymer, which could subsequently be cleared from the body.

However, successful evaluation and optimization of this system requires a more complete understanding of the degradation process *in vivo* and the distinct biodistributions of the degraded and un-degraded polymer populations. Therefore, we have added two fluorophores known to undergo fluorescence resonance energy transfer (FRET). The donor dye, Cy3, was attached to the polymer while the acceptor dye, Cy5, was incorporated into the degradable linker. As such, upon multimerization the FRET pair is strategically separated by the enzymatic cleavage site. Therefore, each cleavage event would also terminate an instance of energy transfer. As a result, the low molecular unimers regenerated upon enzymatic degradation will have a fluorescence profile distinct from their parent multimers.

Upon effective chain extension (confirmed by size exclusion chromatography) the donor fluorescence from direct excitation was noticeably quenched while a second emission peak (corresponding to the emission maxima of the acceptor dye) was observed, both of which are indicative of FRET. Furthermore, extended incubation with the model lysosomal enzyme papain completely removed the acceptor dye's peak such that no FRET was detectable. During the papain incubation, samples were collected at designated time points and their respective fluorescence and SEC profiles were determined.

The degree of FRET was determined by exciting the donor fluorophore and measuring emission from the acceptor fluorophore. The fluorescence signal was found to correlate linearly with the extent of degradation, which was quantified by SEC. This result validates fluorescence as a means to monitor and quantify degradation of these polymers with accuracy equivalent to SEC. However, fluorescence also has the added advantage of being quantifiable both spatially and temporally, facilitating its use for *in vitro* and *in vivo* systems. Specifically, the incorporation of a near-infrared FRET pair in this proof-of-concept could enable non-invasive *in vivo* measurements for independent tracking of degraded and un-degraded polymer populations.

Contact Information:
D. Christopher Radford
chris.radford@utah.edu